

Automatic Skew Control on Container Transshipment Cranes

G. E. Smid*, J.B. Klaassens, H. R. van Nauta Lemke,
A. El Azzouzi[†] and R. van der Wekken[†]
Faculty of Information Technology and Systems
Control Laboratory
Delft University of Technology

Abstract

The jumbo container cranes at the European Container Terminal (ECT) in Rotterdam are subject of a long term study to automate the international seaport and make container handling more efficient.

In this paper we describe the design and simulation of a skew controller that will be used to attenuate the skew motion of the suspended container during transshipment. State feedback control methodology is used for this application. A 3D dynamic model of the container crane was previously developed, and is used here for optimization of the feedback gains.

Keywords : container crane, skew control, state feedback, gantry crane.

1 Introduction

The need for fast and safe loading and unloading container vessels whose service time is to be minimized, requires a control of the crane motion that optimizes the crane's dynamic performance. The two-dimensional cycle is shown in Figure 1 and is divided in three motions: load hoisting, transfer and load lowering. The problems are the reduction of the total time of load transport (time-optimal trajectory control [1], [4]) and reduction of the swing and skew of the container at its end position, including accurate positioning of the load.

During the transport of the load, the planar position is controlled by varying the position of the trolley and varying the length of the four suspension cables. Specific constraints such as maximum torque (which is a maximum acceleration or deceleration of the trolley or load), maximum speed and the existence of obstacles on the quay or in the container vessel, have to be incorporated in the trajectory controller.

A validated math model is necessary for conducting detailed study of the dynamic behavior of the container crane and control schemes. Although several analyses have been made, using nonlinear models [6], [7], further increased complexity has been considered by including the detailed construction of the crane, the stretch in the cables and the influence of wind [5].

The control issues of swing have been addressed thoroughly before. Skew motion is caused by difference in cable length, unsymmetric loading, wind or by interaction of the load with other rigid obstacles.

The selection of the actuator system and control methodology is explained after the introduction of the various options for skew control. Then the state feedback control scheme is explained and the functions for the feedback gains are explained.

*Transportation Equipment Control (TEC)

[†]Siemens Nederland NV. Harbour Transshipment Systems.

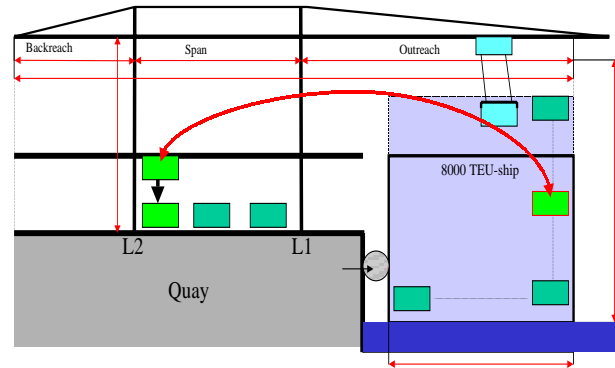


Figure 1: Schematic drawing representing loading and unloading of the Jumbo Container Crane.

The implementation of the control scheme in the 3D model provides the simulation results. Finally, the conclusions are formulated, based on simulation and implementation.

2 Skew Control Methods

A variety of methods are available to influence the skewing motion of a suspended container. They have been discussed by A. Azzouzi in [2] and [3]. Two categories can be distinguished for skew control. Among the *indirect methods* are:

1. Individual cable length control by varying the length of the four cables separately anywhere in the cable loop. For example through individual cable length control by controlling the hoisting drums separately.
2. Skew motion control by applying forces on the container at the trolley. For example by mounting additional diagonal cables between the trolley and the spreader. Or by moving the hoisting pulleys on the trolley in the trolley motion direction, anti-symmetrically. In this way, forces are applied on both sides of the container.

Direct methods consist of skew motion and center of gravity control at the side of the spreader. Among the direct methods are:

3. The application of flywheels on the spreader
4. Mounting propellers on the spreader
5. Shifting of the pulleys for the hoisting cables on the spreader to control the mass distribution.

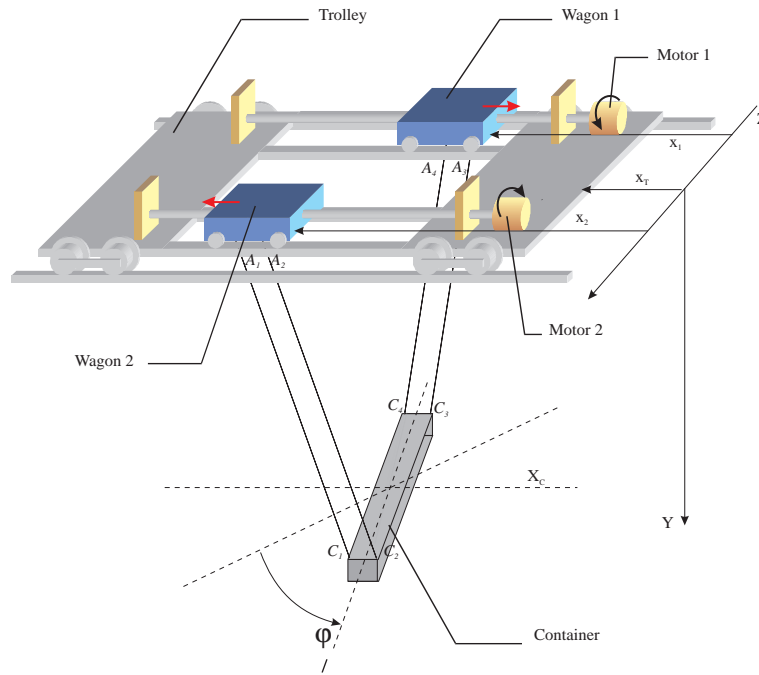


Figure 2: Mechanical construction of the skew actuators.

6. Use of linear drives, to shift the container in the mounts of the spreader, also in order to control the mass distribution
7. Add additional mass to the spreader, to correct for unbalanced loading of the spreader.

The direct methods are generally more efficient, but less robust than the indirect methods. An important consideration for applying a particular method of skew control is the claimed patents on specific schemes.

3 Skew Control Actuator System

Considering controllability and robustness, and the commercial protection, the indirect method 2 suits best to attenuate container skewing motion. Notice that the trimming of the container, which is current practice in the container crane operation, corresponds with method 1 for passive skew control. On the newest cranes this active skew actuator is realized by two anti-parallel movable hoist sheave units on the trolley in the trolley direction. The sheave units will be controlled by the real-time active skew controller integrated in HIPAC¹, through the DC Masterdrive of the Siemens PLC.

The actuator is called a “wagon”. Its mechanical construction is given in Figure 2. Two linear translational wagons can be moved by a reversible gear. The hoisting pulleys are mounted on the wagon units. The dynamic non-linear model of the actuator with limitations on the position x_W , the velocity \dot{x}_W and the acceleration \ddot{x}_W is given in Figure 3.

4 The Concept of Skew Control

The block diagram of the skew feedback control system is given in Figure 4. The measured value of the skew angle, ψ

¹Highly Intelligent Pendulum Automatic Controller (HIPAC) is a product of Siemens Nederland NV.

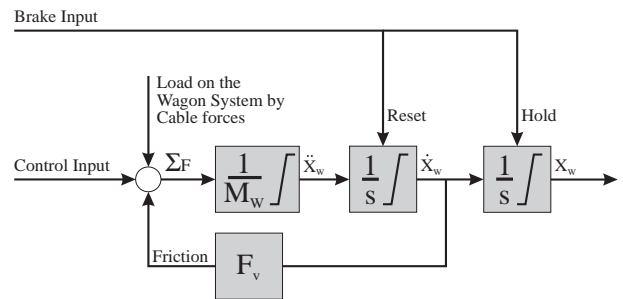


Figure 3: The diagram of the non-linear dynamic model of the skew actuator.

is compared with the defined desired reference value. Normally, i.e. without disturbances like wind, this reference value equals zero.

The error signal ϵ_ψ is fed to a controller using the gain parameter K_1 , giving an actuation reference value for the positioning of the wagon. This wagon system is implemented in a well-known way, making use of the velocity feedback loop (\dot{x}_W) and design gain parameters K_3 and K_4 .

To improve the dynamic behavior of the skew control system (especially to increase the bandwidth of the system), the controller in the forward path of the skew control is replaced with a separate skew velocity feedback loop, $\dot{\psi}$ and gain parameter K_2 . This design method omits an integral action. In a later stage of the design, the possibility is available to add an integral action in the forward loop, so that the accuracy in the last part of the positioning can be improved (the I-action may easily be defined as a function of the positioning error).

5 State Feedback Control

As part of his thesis, N. Schouten discussed the advantages and disadvantages of several control strategies [8]. In his conclusion on the choice of the *state feedback control*

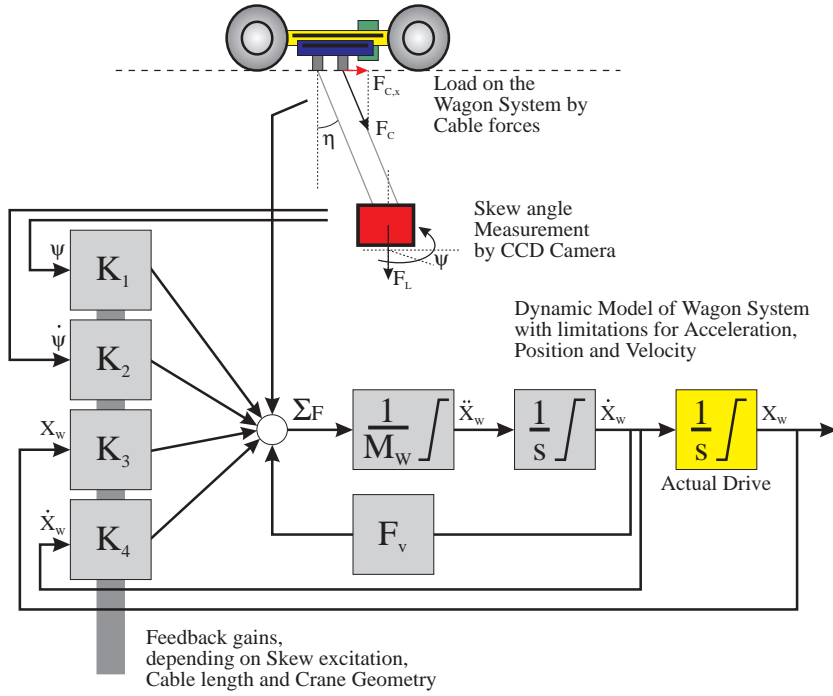


Figure 4: Diagram of the control model and the dynamic model of the skew actuator.

concept, he emphasizes on the generality and robustness of the state feedback control. When looking for an optimal solution for the state feedback controller, the feedback gains should depend on the state of the system:

- Lower gains for large errors, so that the system is not controlled beyond its limits,
- Higher gains for approaching end position, in order to minimize the error.

Full state feedback control allows the designer to place the poles of the model anywhere in the complex plane without adding dynamic states to the system. With a limited state feedback control, the designer is not anymore able to place each pole individually.

The above state feedback skew controller for container cranes can be described by the following set of equations:

$$F = K_1(f)\psi + K_2(f)\dot{\psi} + K_3(f)x_w + K_4(f)\dot{x}_w \quad (1a)$$

$$\ddot{x}_w = \frac{1}{M_w}F \quad (1b)$$

$$\dot{x}_w = \dot{x}_w(0) + \int_{t_0}^t \ddot{x}_w dt \quad (1c)$$

where F represents the *virtual force* for the desired skew actuator motion, and $K_i(f)$, $i = 1, \dots, 4$ represents the *gains* of the state feedback controller. The skew angle and skew rate are denoted by ψ and $\dot{\psi}$, and the wagon position and speed with x_w and \dot{x}_w , respectively. The gains are dependent on the state of the system. The force F will be transformed into the desired actuator acceleration and the acceleration is then integrated to the desired actuator speed $\dot{\psi}$, being the output of the controller. In order to save the motor drive from overheating, a moving-average filter is implemented in the controller for smoothing the acceleration.

6 Optimal Control Design

The next problem is to find the controller gains $K_i(f)$. Parametric optimization is used to find a set of controller design parameters $C = \{K_1, K_2, \dots, K_n\}$, which can be defined as optimal. In the case of the skew actuator system, the objective function, $f(C)$, to be minimized, may be subject to constraints in the form of equality constraints $G_i(C) = 0$ ($i = 1, \dots, m_e$), inequality constraints $G_i(C) \leq 0$ ($i = m_e + 1, \dots, m$), and parameter bounds C_l, C_u .

A General Problem (GP) description is stated as

$$\min_{C \in \mathbb{R}^n} f(C), \quad (2)$$

$$\text{subject to: } G_i C = 0, \quad i = 1, \dots, m_e$$

$$G_i(C) \leq 0, \quad i = m_e + 1, \dots, m \quad (3)$$

$$C_l \leq C \leq C_u$$

where C is the vector of controller design parameters (i.e. the feedback gains), ($C \in \mathbb{R}^n$), $f(C)$ is the objective function that returns a scalar value ($f(C) : \mathbb{R}^n \rightarrow \mathbb{R}$), and the vector function $G(C)$ returns the values of the equality and inequality constraints evaluated at C ($G(C) : \mathbb{R}^n \rightarrow \mathbb{R}^m$).

Quadratic Programming (QP) concerns the minimization of a quadratic objective function that is linearly constrained. For QP problems, reliable solution procedures are readily available.

In the case of the skew control problem, the performance criterion can be formulated as the time quadratic penalty of the skew motion angle error with the desired skew angle, i.e.

$$f(C) = \int_t \psi^2 dt \quad (4)$$

The skew angle $\psi(t)$ is found by simulating the crane model with a set of initial conditions for a period of time, and

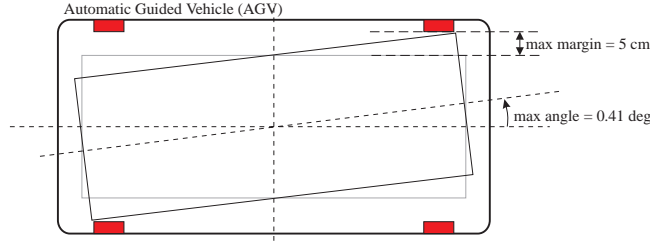


Figure 5: Maximum skew angle in relation to the positioning accuracy of the container on the AGV (5 cm error).

recording the states of the system. The model in this case is described in detail in [5].

The inequality constraints are defined as the physical actuator limitations plus the overshoot. In other words, the physical limitations may never be exceeded, and the overshoot must be less than the allowable skew angle margin. In equations these inequality constraints are formulated as follows:

$$G_1(C) = \max(|x_W|) - 0.5 \quad (5)$$

$$G_2(C) = \max(|\dot{x}_W|) - 0.5 \quad (6)$$

$$G_3(C) = \max(|\ddot{x}_W|) - 1.5 \quad (7)$$

$$G_4(C) = \max(\psi) - 0.035 \quad (8)$$

The maximum allowable overshoot of 0.035 rad (0.41 deg) represents 10 cm overshoot on a 13.76 m (45 ft) container, as shown in Figure 5. The constraint on the overshoot must be applied with care. The optimization algorithm is very strict with the defined constraints. In some cases, for large skew angle, short pendulum length and small inertias, the container skew will have overshoot anyway. For these cases the optimization procedure will quit, with the message that it cannot find a solution to the problem.

The optimization process has been conducted for different cable lengths and different inertias, since these parameters are of influence on the harmonic skew frequency.

From the optimization results, functions for the gains K_i can be found, depending on cable length and load inertia. The gains are not a function of the load mass M . The mathematical derivation for a pendulum does not identify any relation of the pendulum time and the load mass.

The settling time is the first time that a maximum size container (45 ft \approx 13.76 m) will make a skew motion with an amplitude which is smaller than the positioning space margin on the AGV² (or the last time when the amplitude exceeds the margin). This margin is 10 cm, corresponding with a maximum skew angle

$$\psi_{\max} = \frac{0.10}{13.76} \frac{180}{\pi} \approx 0.4167 \text{ deg.} \quad (9)$$

The settling time is thus defined as

$$T_s = \max_t \left\{ \|\psi(t)\| > 0.4167 \right\} \quad (10)$$

7 Simultaneous Skew and Swing

Container swing is a natural harmonic translational motion of the container relative to the trolley. When the container is

²Transport of the containers between the stacking area and the container cranes is done with Automatic Guided Vehicles (AGV).

suspended with four parallel cables, the container list angle θ (about the y -axis) is not affected by the swing. This is the case when the distance between the hoisting pulleys $A_1 - A_2$ (See Figure 2) on the trolley equals the distance between the hoisting pulleys $C_1 - C_2$ on the spreader. The motion dynamics are then decoupled within a certain error boundary, because of the perpendicular motion direction: the swing motion is about the y -axis in trolley geometry, while the skew motion is about the z -axis in container.

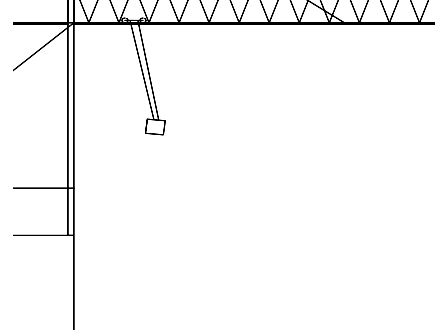


Figure 6: Effect of non-parallel cable configuration on the container list motion.

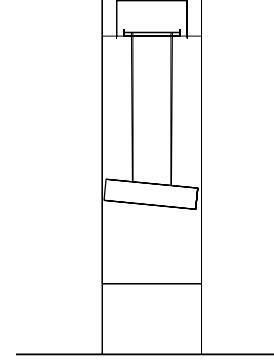


Figure 7: Effect of load shift on the suspended container.

When the distances between the hoisting pulleys on the trolley and on the spreader differs, the distances between the hoisting points $A_i - C_i$, for $i = 1 \dots 4$ on the trolley and spreader will vary with the swing angle. As a result, the container will list (i.e. rotate about the y -axis) to make up for the difference in this distance. The list angle caused by the swing can be expressed as a function of the difference in pulley distances on the trolley and the spreader, and the swing angle η as:

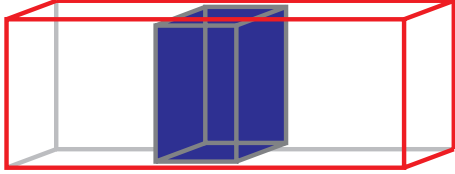
$$\theta = \arcsin \left(\frac{A_2 - A_1}{C_2 - C_1} \sin(\eta) \right) - \eta \quad (11)$$

The effect is shown in Figure 6. The list motion is slightly attenuated with increasing load mass, and with low center of gravity, due to the compensating effect of cable stretch.

Thus the difference in the width (in x -direction) between the pulleys on the spreader and on the trolley cause the container to make a list motion when there is sway. Because of the list angle, the skew and sway motion are no longer perpendicular in space. This effect perturbs the attenuation of the skew control and introduces dependency from the skew angle of the container swing.



(a) Large inertia with the mass away from CG



(b) Small inertia with the mass close to CG

Figure 8: Different inertias for the same mass under symmetrical loading condition.

Further reading on the crane constructions can be found in [9].

8 Inertia

A homogeneous weight distribution for a 3D rectangular shape is written as

$$\begin{pmatrix} I_x \\ I_y \\ I_z \end{pmatrix} = \frac{1}{12} M \begin{pmatrix} w^2 + h^2 \\ l^2 + h^2 \\ l^2 + w^2 \end{pmatrix} \quad (12)$$

with length l , width w , and height h being the shape dimensions of the container in the x , y and z -direction respectively.

Figure 8 shows how the inertia should be understood for different loading of the same shape.

It may be obvious from a mechanical dynamic point of view that the inertia I_y is an important parameter in the controller configuration. The problem now is, how the inertia should be estimated from an unknown container. The only clue we would have is the skew harmonic period time, with respect to the mass and the pendulum length.

From the fact that the container dimension appears in the formula for the inertia in Equation 12, we can conclude that the variation in load inertia reflects the different sizes of containers (assuming homogeneous weight distribution). The inertia will thus be made a function of the container size.

The control algorithm assumes an inertia factor λ , which represents the ratio of the sway period and the skew period for the same pendulum length. The inertia factor can be computed by noting that a homogeneous loaded container with sizes $3 \times 10.9716 \times 3$ m represents the inertia factor 1. λ can be calculated with

$$T_{skew} = 2\pi\lambda\sqrt{\frac{L}{G}} \quad (13)$$

by plugging in the measured pendulum length L and measuring the skew time period T_{skew} .



Figure 9: Simulation results are shown in VRML

9 Unsymmetrical Load

One of the successes of world-wide container transportation is that container shipping can be standardized. Generally the type of content of a container is known, but not the weight distribution. Eventhough international regulations prescribe a maximum weight shift of 10% from the geometric center, it is important to consider the robustness of the skew controller in this respect.

Obviously, for a container with steel plates, the Center of Gravity (CG) will be low, and for an empty container it will be high. A container that is loaded sideways will trim, see Figure 7, which will result in a difference pendulum lengths for the left and right side of the container and thus introduce skew.

10 Simulation

The mathematical formulation for the container crane model and the skew controller have been implemented in MATLAB. The simulation results are displayed using a VRML representation of the crane, as shown in Figure 9.

In a scenario where the container is moved from the ship to the shore under skew motion, and lowering takes place during the horizontal transport, the controller shows good performance for attenuating skew motion (Figure 11).

This simulation setup has been used for studying the behavior of the system under numerous operating conditions and scenarios.

11 Conclusion

Mass

In this chapter we have seen that the skew attenuation performance of the controller is not dependent on the load mass, the cable stiffness or the swing motion. When the actuator is not in saturation, the performance is also independent of the amplitude of the skew motion when the controller is activated. Furthermore, when the center of gravity is within the



Figure 10: Picture of the side of the container crane

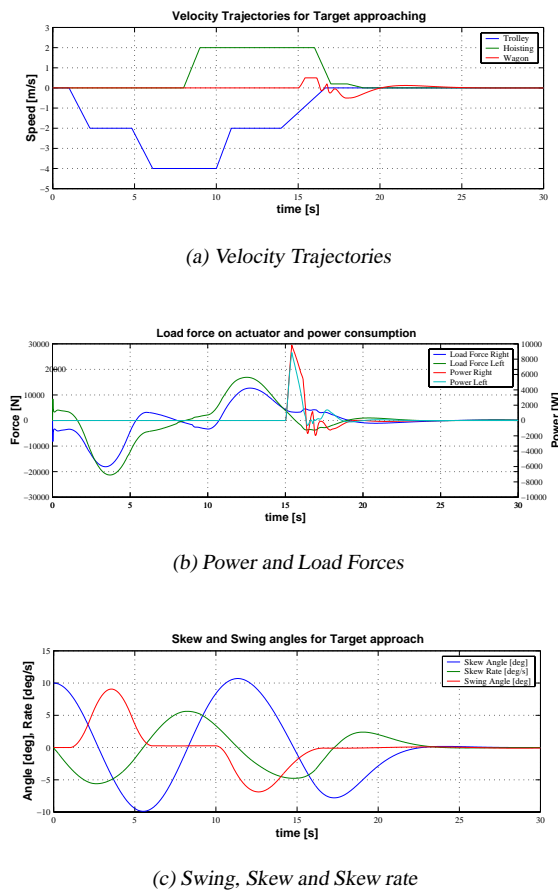


Figure 11: Simulation results of approaching the end position by combined deceleration and hoisting with skew control.

restricted boundary region (according to the regulations for container transportation), then the skew control performance is also independent on the location of the center of mass.

Inertia

However, the pedulum length and the inertia are both the critical parameters for configuring the controller optimally. The error of the measured pedulum length has proven to be of small influence. Also the error on the inertia shows only a small decrease in performance. The inertia however, will still be a guess, since no sensors provide a value for this parameter. The spreader with an empty container is assumed to average to a homogeneous weight distribution. The additional load of the contents of the container is estimated to be homogeneously distributed over the container.

Wind

In simulations it has also been shown that a container which experiences a strong wind gust (a wind gust which would initiate a skew motion of 15 deg on a container at a pendulum length of 35 m) is effectively reduced to neutral by the controller.

Noise

Sensor noise and interruptions have been shown to deteriorate the performance of the control scheme. Generally, the control algorithm will be as good as the sensor inputs. In other words, the controller will not increase the accuracy of the overall system. Simulations have shown that the controller will still perform under noise and interruptions of the sensor skew signal.

Motor Drive Dynamics

The control loop for the electrical drives of the skew actuators which are responsible for tracking the speed trajectory, have a sampling rate which is at least one order more than that of the HIPAC controller hardware. Transition time from one speed setpoint to the next is assumed to be less than the sampling interval time of the HIPAC controller, taking into account that successive velocity setpoint cannot differ more than the physical acceleration limit of the drives.

References

- [1] J. W. Auernig and H. Troger. Time optimal control of overhead cranes with hoisting of the load. *Automatica*, 23(4):437–447, 1987.
- [2] A. El Azzouzi. Skew control jumbo container crane jcc-2000. Technical report, Technische Universiteit Delft, werkeenheid regeltechniek., 1998. Internal Technical report for Siemens Nederland N.V.
- [3] K. O. Boinov. Modeling and control of skew. Technical report, Delft University of Technology, Control Laboratory, 1999.
- [4] P. Hippe. Time optimal control of an overhead crane. *Regeltechnik und Prozess-Daten arbeitung*, 18(8):346–350, 1970.
- [5] J. B. Klaassens, G. Honderd, A. El. Azzuzi, Ka C. Cheok, and G. E. Smid. 3d modeling and visualization for studying controls of the jumbo container crane. In *Proceedings of the American Control Conference*, San Diego, June 1999.
- [6] A. J. Ridout. Anti swing control of the overhead crane using linear feedback. *Journal of Electrical and Electronic Engineering*, pages 17–26, 1989.
- [7] Y. Sakawa and Y. Shindo. Optimal control of container cranes. *Automatica*, 18(3):257–266, 1982.
- [8] N. Schouten. Time optimal controller design for the jumbo container crane. Master's thesis, Delft University of Technology, 1999.
- [9] J. Verschoof. *Cranes. Design, Practice and Maintenance*. Professional Engineering Publishing, 1999. ISBN 1 86058 130 7.